Transducer model produces facilitation from opposite-sign flanks

Joshua A. Solomon [a,*], Andrew B. Watson [b], Michael J. Morgan [a]

[a] *Institute of Ophthalmology, Bath Street, London EC1V 9EL, UK*
[b] *NASA/Ames Research Center, Mail Stop 262-2, Moffett Field, CA 94035-1000, USA*

Abstract

Small spots, lines and Gabor patterns can be easier to detect when they are superimposed upon similar spots, lines and Gabor patterns. Traditionally, such facilitation has been understood to be a consequence of nonlinear contrast transduction. Facilitation has also been reported to arise from non-overlapping patterns with opposite sign. We point out that this result does not preclude the traditional explanation for superimposed targets. Moreover, we find that facilitation from opposite-sign flanks is weaker than facilitation from same-sign flanks. Simulations with a transducer model produce opposite-sign facilitation. © 1998 Elsevier Science Ltd. All rights reserved.

Keywords: Masking; Facilitation; Lateral; Spatial

1. Introduction

Masking and facilitation[1] refer, respectively, to a decrease and an increase in the detectability of one pattern (the target) caused by the presence of another pattern (the mask). Traditionally, masking and facilitation have been thought to arise from the nonlinear response of neurones sensitive to local contrast (Nachmias & Sansbury, 1974; Stromeyer & Klein, 1974; Legge & Foley, 1980; Legge, 1981; Wilson, McFarlane & Phillips, 1983; Ross & Speed, 1991; Foley & Boynton, 1993; Yang & Makous, 1995). In such transducer models, a target is detected when its presence causes a criterion change in the neurones' responses. For small contrasts, the response is accelerating. For large contrasts, the response is decelerating. Thus detection threshold can be lower for low-contrast masks than no-contrast masks and it can increase with mask contrast for high mask contrasts (see Fig. 1).

Recently, a number of investigators have reported facilitation arising from nonoverlapping patterns. Gabor patterns can be easier to detect when flanked by similar Gabor patterns (Polat & Sagi, 1993, 1993; Zenger & Sagi, 1996); small spots can be easier to

detect when flanked by lines and edges (Dresp, 1993; Morgan & Dresp, 1995) and lines can be easier to detect when flanked by small spots (Yu & Levi, 1997) and other lines (Kapadia, Ito, Gilbert & Westheimer, 1995).

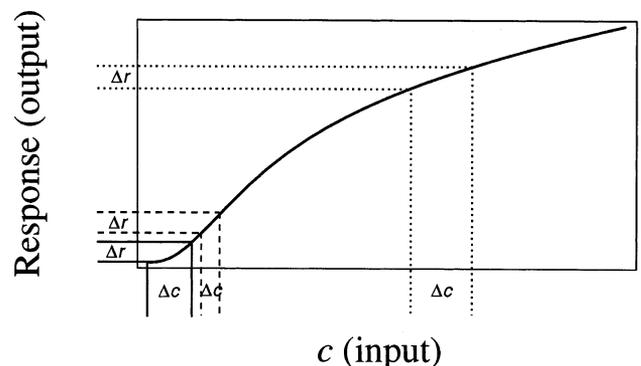Most of these investigators reject transducer models of masking and facilitation (Polat & Sagi, 1993;

Fig. 1. Transducer model of masking and facilitation. When response differs by more than some criterion Δr, the target can be detected. Consider absolute threshold, i.e. when no mask is present. Here, it is represented as the distance between the two vertical solid lines. The same change in response that produces absolute threshold also produces threshold for every other masking contrast. The dashed lines show that for certain masking contrasts, Δc is smaller than absolute threshold. This accounts for facilitation. The dotted lines show that for other masking contrasts, Δc is larger than absolute threshold. This accounts for masking.

---

* Corresponding author. Fax: +44 171 6086846; e-mail: j.solomon@ucl.ac.uk.
[1] In this paper only simultaneous masking and facilitation (i.e. when target and mask appear simultaneously) are considered.

Zenger & Sagi, 1996; Yu & Levi, 1997). Their main argument stems from the result that facilitation occurs even when target and flanks have opposite-sign contrast. Morgan and Dresp (1995) concur that such a result would be problematic for transducer models, but they failed to obtain it in two out of three observers. Kapadia et al. (1995) do not consider transducer models. Polat and Sagi (1993) further argue that, since the range of facilitation is much larger than the target, facilitation cannot be attributed to mechanisms sensitive to local contrast.

We argue that transducer models of masking and facilitation do predict facilitation arising from flanks of opposite sign. First, consider a masking experiment where the mask and target have opposite sign but are otherwise identical. The target causes an increase in the response of the neurone most sensitive to it. The target also causes a decrease in the response of the neurone most sensitive to the mask. Both neurones can contribute to detection of the target. If the neurone most sensitive to the mask is in its accelerating region, then facilitation will occur.

The same logic can be applied to cases where the mask flanks the target. Again, consider two neurones: one sensitive to the target (with a receptive field centred on the target); the other sensitive to the flank, with a receptive field between this flank and the target. The neurone sensitive to the target is responsible for absolute threshold, as indicated in Fig. 1. When target and flank have opposite sign, introduction of the target will reduce the response of the neurone sensitive to the flank. If this neurone is responding in its accelerating region, then facilitation will occur.

Furthermore, we argue that there is no theoretical reason why a neurone cannot be sensitive to both target and flank, regardless of their separation. Using Gabor patterns, Polat and Sagi (1993) report that facilitation disappears when the target/flank separation is between six and twelve wavelengths (i.e. 6 and 12λ). Fig. 2 illustrates that a single receptive field can overlap both target and flank, even when separated by 6λ.

The purpose of this study was 2-fold. First, we wanted to confirm and quantify the amount of facilitation arising from opposite-sign, flanking Gabor patterns. Polat and Sagi (1993) claim that opposite-sign flanks produce 'practically the same results' as same-sign flanks, but they provide no data on this issue. Zenger and Sagi (1996) used flanks with signs opposite to each other; one flank always had the same sign as the target. Such flanks would not stimulate neurones centred on the target, but, as we argue here, other neurones can contribute to detection. In particular, the facilitation they report could be due to neurones positioned between the target and the same-sign flank. Second, we wanted to demonstrate a transducer model that produces facilitation from opposite-sign flanks.
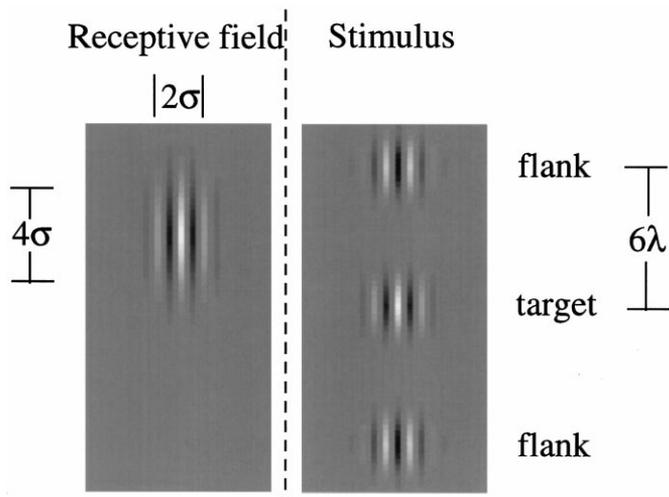

Fig. 2. Facilitation from opposite-sign flanks. A receptive field with a 2:1 aspect ratio overlaps with both the upper flank and the target. The neurone's response to the flank and target together is smaller than its response to the flank alone. If the neurone is in the accelerating region of its response, then facilitation can occur.

2. Experiment

Polat and Sagi (1993) found maximal facilitation arising from (same-sign) flanks separated from the target by 3λ. Our methods were designed to duplicate theirs as closely as possible. In addition, we used flanks separated from the target by 2 and 4λ, at a variety of contrasts. We used horizontal rather than vertical Gabor patterns to reduce limitations of monitor bandwidth.

2.1. Methods

Two of the authors served as observers. Both had normal or corrected-to-normal vision and were highly practiced in similar experiments. Stimuli were displayed with gamma correction on a monochrome CRT. Maximum and minimum display luminances were 54 and 0.0 cd m^{-2}, respectively. The background luminance was held constant at 27 cd m^{-2} and the frame rate was 66.7 Hz. Display resolution was 30.3 pixels/cm. Observers viewed the screen from 99 cm, resulting in an effective visual resolution of 53 pixels/°. The Psychophysica/ Cinematica (Solomon & Watson, 1996; Watson & Solomon, 1997a) software used in these experiments is available on the internet at http://vision.arc.nasa.gov/ mathematica/psychophysica.html.

The target was a horizontal circular cosine phase Gabor pattern; the product of a sinusoidal grating and a Gaussian blob. The grating had a spatial frequency of 13 cycles/°. At half height, the Gaussian window contained 0.52 square periods. Flanks were in minus cosine phase but otherwise identical to the target, positioned 0.15, 0.225 or 0.375° (2, 3 or 4λ) to the right and left of the target (see Fig. 3 legend).

Each trial consisted of two consecutive stimulus presentations, one of which contained the target. When ready, the observer pushed a key to initiate the trial sequence: a fixation spot disappeared, there was a brief pause (randomised within a range of 360 ± 270 ms), a stimulus presentation for 90 ms, another pause (randomised within a range of 540 ± 270 ms), a second 90 ms stimulus presentation and a final pause of 360 ms before the fixation spot returned.

Each stimulus presentation was marked by four high contrast spots positioned at the corners of a 0.71° square centred upon fixation. The observer identified the stimulus presentation containing the target by pressing one of two keys. A correct choice was followed by a low frequency tone; an incorrect choice by a high frequency tone. Psychophysical estimates were obtained with a version of the QUEST procedure (Watson & Pelli, 1983) which converged to the 82%—correct threshold for detecting the target in the presence of the flanks.

Each session consisted of 64 trials in which flank position and contrast were fixed. We express contrast in decibels (dB), where $dB(contrast) = 20 \log_{10}(contrast)$ (0 dB implies that the pattern reaches either the minimum or maximum display luminance). Five mask contrasts were used in different sessions: 0, -4, -8, -12, and -16 dB. Zero flank contrast ($-$infinity dB) was also used. Observers completed three series of (three masks × five contrasts + zero contrasts equals) 16 sessions. The order of mask contrast (including zero) was randomised.

Because the results of this experiment indicate only weak facilitation arising from opposite-sign flanks, we sought to confirm the amount of facilitation arising from same-sign flanks as reported by Polat and Sagi
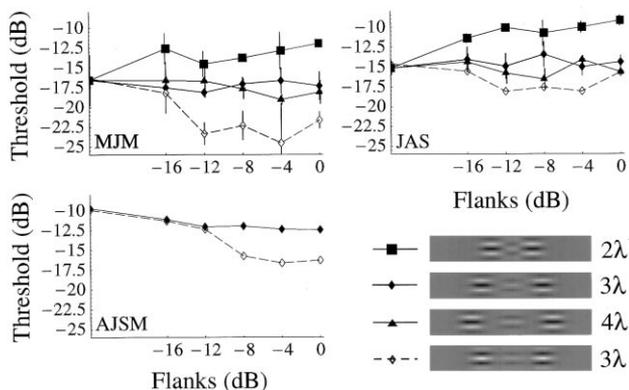
(1993). MJM repeated the procedure using same-sign flanks separated from the target by 3λ. JAS and another subject (an experienced psychophysical observer) had run an experiment with same-sign flanks as part of a pilot study. The results of the pilot study are discussed in conjunction with the results of the present study, below. Methods for the pilot study were identical to methods for the current study except that 128 trials at each flank contrast were interleaved at random throughout a single session. AJSM also completed a (128 trials × six contrasts, including $-$infinity dB, equals) 768 trial session using opposite-sign flanks separated from the target by 3λ.

2.2. Results

Results are shown in Fig. 3. Absolute threshold (flank contrast at $-$infinity dB) is plotted on each ordinate. Points above absolute threshold indicate masking; points below indicate facilitation. Results from observers MJM and AJSM indicate weak facilitation from opposite-sign flanks. Specifically, MJM's absolute threshold is 2.5 dB higher than his threshold with -4 dB opposite-sign flanks separated from the target by 4λ. A one-tailed t test confirms that the two thresholds are different, $P < 0.005$. AJSM's absolute threshold is 2.7 dB higher than her threshold with 0 dB opposite-sign flanks separated from the target by 3λ. At no contrast did opposite-sign flanks produce significant facilitation for JAS.

Same-sign flanks were much better facilitators than opposite-sign flanks at all contrasts. At -8 dB, our methods replicated those of Polat and Sagi (1993) exactly (except that we used horizontally flanked horizontal Gabor patterns instead of vertically flanked vertical Gabor patterns) and like Polat and Sagi, we found that these conditions produced an average of 5 dB facilitation.

3. Transducer model

We attempted to fit a transducer model to the data of Polat and Sagi (1993) and to our own data. Responses of neurones with Gabor-pattern receptive fields were simulated by transduction of the output of a linear filter. For simplicity, we used a single filter, matched to the spatial frequency and orientation of the Gabor patterns which comprise the input images. Let x and y be the spatial dimensions perpendicular and parallel to this orientation, respectively. Let f_0 be the spatial frequency. The filter can then be specified in the frequency domain:

$$G(\omega_x, \omega_y) = e^{-\frac{(f_0 - \omega_x)^2}{2\sigma_x^2} - \frac{\omega_y^2}{2\sigma_y^2}}. \tag{1}$$

Fig. 3. Threshold vs. flank contrast for three subjects. Absolute threshold (flank contrast at $-$infinity dB) is plotted on each ordinate. Opposite-sign flanks were separated from the target by 2, 3 and 4λ of the carrier grating (i.e. 2, 3 and 4λ). Same-sign flanks were separated from the target by 3λ. Target/flank geometry is shown on the lower right, with target contrast at -10 dB and flank contrast at 0 dB. Error bars indicate S.E. of the mean of three measurements. Same-sign flanks can lower threshold more than opposite-sign flanks.

Table 1
Parameter values used for fitting the data of Polat and Sagi (1993) (Fig. 4) and MJM's opposite- and same-sign data (Fig. 5)

Model parameters		Parameter values	
		Fig. 4	Fig. 5
d	Criterion for discrimination	0.01196	0.01538
p	Excitatory exponent	3.043	3.003
q	Inhibitory exponent*	$p-0.3$	$p-0.3$
b	Saturation constant	2.208	2.190
σ	Filter spread across target frequency f_0 *	$0.258\, f_0$	$0.258\, f_0$
σ	Filter spread orthogonal to target frequency f_0	$0.195\, f_0$	$0.202\, f_0$
β	Minkowski exponent	4.993	9.536

Parameters with an asterisk (*) were fixed.

The simulated area was a square with 64 pixels on each side. There were four pixels per period of the Gabor patterns which comprised both the images displayed to our observers (see Methods) and the input images for the simulations.

The intensity of each pixel in the real part of a filtered image represents the input $c_{\{x, y\},0}$, to a neurone with an even-symmetric receptive field centred on the corresponding pixel of the input image. The intensity of each pixel in the imaginary part of a filtered image represents the input $c_{\{x, y\},\pi/2}$ to a neurone with an odd-symmetric receptive field centred on the corresponding pixel of the input image. The relationship between input $c_{\{x, y\},\phi}$ and response $r_{\{x, y\},\phi}$, is given by the equation:

$$r_{\{x, y\},\phi} = \frac{c_{\{x, y\},\phi}^{p}}{c_{\{x, y\},\phi}^{q} + b^{q}}. \tag{2}$$

Transducer functions of this form appear in the models of Stromeyer and Klein (1974), Legge and Foley (1980) and Ross and Speed (1991).

Potentially, each neurone will respond differently to the two input images (mask + target and mask alone). These response differences are combined to produce a metric for discrimination d:

$$\left(\sum_{x, y, \phi} \left| {}_1r_{\{x, y\},\phi} - {}_2r_{\{x, y\},\phi} \right|^{\beta} \right)^{1/\beta} = d. \tag{3}$$

Detection occurs when d reaches a criterion. All of the model parameters are summarised in Table 1.

Using Mathematica's FindMinimum routine (Wolfram, 1996), this transducer model was fit to the data of Polat and Sagi (1993), optimising the parameters σ_y, d, b, p and β. σ_x was set to the frequency spread of the target. It is necessary to maintain $q = p - 0.3$ in order to produce masking functions (threshold (dB) vs. contrast (dB)) that have the correct asymptotic slope (Watson & Solomon, 1997b). The results of this fit are illustrated in Fig. 4. Parameter values are summarised in Table 1.

Polat and Sagi (1993) found masking when same-sign flanks were separated from the target by 0 or 1λ; they found facilitation when the target/flank separation was 3 or 6λ. The transducer model behaves similarly: when flanks are close they impair detection of the target; when flanks are far they facilitate detection of the target. However, the model does not fit all of their data exactly. Its absolute threshold is too low and its threshold at 6λ is too high. To put it another way, the model predicts too much masking at 1λ and insufficient facilitation at 3 and 6λ. Greater facilitation at larger separations is impossible without greater masking at smaller separations.

To illustrate the model's behaviour with opposite-sign flanks, we selected one set of data (MJM's) and fit the transducer model to it. The results are illustrated in Fig. 5 and the parameter values are summarised in Table 1. Both MJM and the model exhibit facilitation from same-sign flanks, but whereas MJM shows a maximum facilitation of nearly 8 dB (-4 dB flanks), the model's maximum facilitation is only 3 dB. Both MJM and the model exhibit facilitation from opposite-
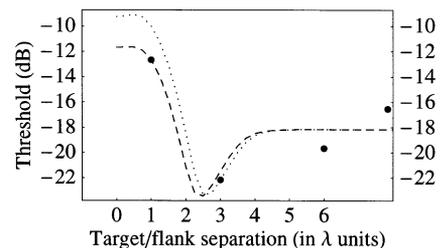

Fig. 4. Fitting the data of Polat and Sagi (1993). Points show performance averaged across observers. At a target/flank separation of 1λ, the same-sign flanks had a contrast of -10.5 dB; at separations of 3 and 6λ, flank contrast was -8 dB. Absolute threshold is shown on the right ordinate. Dashed and dotted curves show the best fitting transducer model applied to -10.5 dB and -8 dB flanks, respectively. Root-mean-square error (RMSE) of the fit is 1.06 dB. The model shows masking from nearby flanks and facilitation from farther flanks.
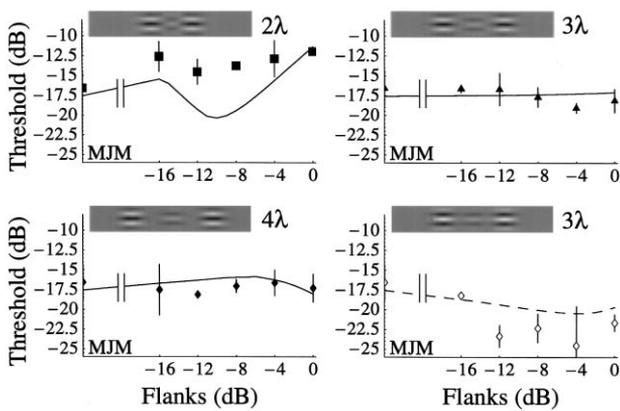
Fig. 5. Fitting MJM's opposite- and same-sign data. Filled boxes, diamonds and triangles show MJM's thresholds with opposite-sign flanks at separations of 2, 3 and 4λ, respectively. Open diamonds show MJM's thresholds with same-sign flanks at 3λ. The transducer model was fit to all of these data simultaneously. RMSE of the fit is 2.44 dB. The model shows facilitation from opposite-sign flanks, but its overall fit is poor.

4. Discussion

The study of masking and facilitation has recently been extended by reports of facilitation arising from non-overlapping patterns (Dresp, 1993; Polat & Sagi, 1993, 1994; Kapadia et al., 1995; Zenger & Sagi, 1996; Yu & Levi, 1997). Yet we believe that rejection of a traditional explanation for these results has been premature. We have demonstrated that the main evidence
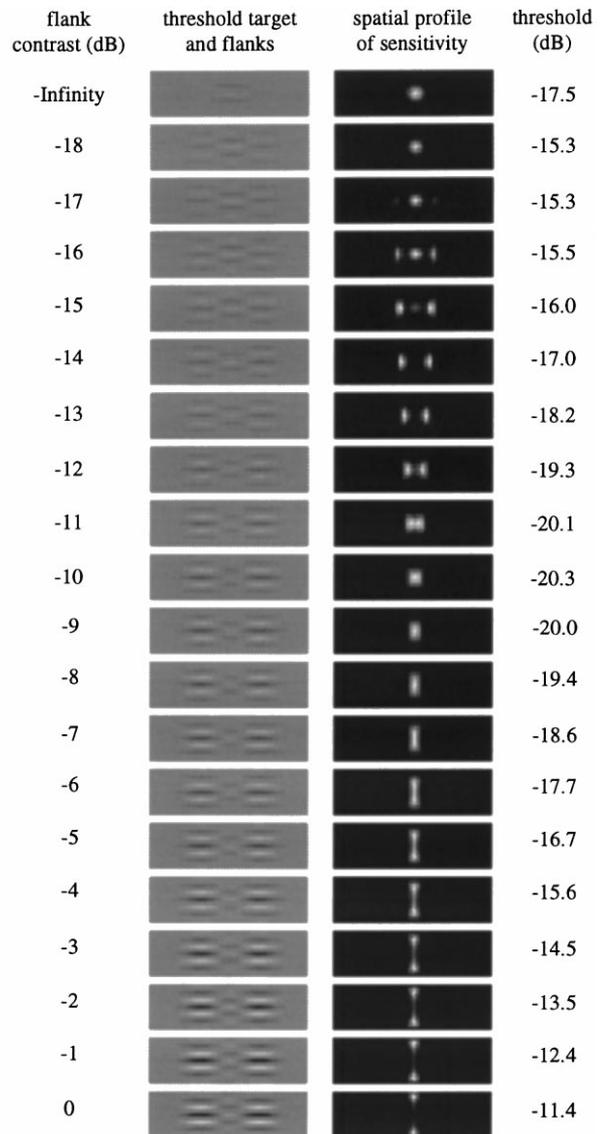
sign flanks too. For MJM this occurs at 4λ; for the model it is greatest at 2λ.

Note that for certain opposite-sign masks (particularly at 2λ) the model's masking function is triphasic; threshold initially increases with masking contrast, then decreases below absolute threshold, then increases again. The initial increase has been termed the 'bumper effect' (Bowen & Cotton, 1993) and has been shown to occur psychophysically (Yang & Makous, 1995). As explained in the Introduction, absolute threshold is mediated primarily by the neurone most sensitive to the target. For small flank contrasts, the target will require additional contrast (over and above that of absolute threshold) to overcome the negative input arising from opposite-sign flanks. This causes the bumper. As flank contrast continues to rise, other neurones will begin to respond in their accelerating regions, causing facilitation (see the Introduction). At high flank contrasts most neurones sensitive to the target will be responding in their decelerating regions, causing masking.

Fig. 6 illustrates how the model's spatial sensitivity changes with the contrast of opposite-sign flanks at 2λ. Threshold targets are shown with a range of flank contrasts. Next to each stimulus the relative sensitivity of neurones at each pixel (i.e. $\Sigma_\phi |_1 r_{\{x, y\}, \phi} - {}_2 r_{\{x, y\}, \phi}|^\beta$ is plotted as an intensity. At absolute threshold, the model's peak sensitivity is centred on the target. At −16 dB threshold begins to drop and there are two new peaks of sensitivity, located between the target and the flank centres. As flank contrast continues to rise, the most sensitive neurones (those responding in their accelerating regions) will be located farther and farther from the flank centres.

Fig. 6. Spatial profiles of the model's sensitivity. For each of 20 flank contrasts, two images are shown. In the first the target appears at threshold (as determined by the traditional model, fit to MJM's data (see Fig. 5)) amidst opposite-sign flanks. Target/flank separation is 2λ. In the other image relative contributions of each pixel toward detection are plotted as intensities. Pixels near the centre of the target make the strongest contributions toward detection when flanks are absent. When flanks begin to cause facilitation, the pixels which make the strongest contribution toward detection are located between the centre of the target and each flank.

used for this rejection, facilitation from opposite-sign flanks, is consistent with transducer models. Moreover, we have shown that, when compared with facilitation arising from same-sign flanks, facilitation from opposite-sign flanks is very weak.

We have run simulations with a transducer model. It predicts masking from nearby flanks and facilitation from farther flanks, including opposite-sign flanks, but its overall fit to the data is poor. A transducer model that used more neurones with various preferences for orientation might produce a better fit to the data. Facilitation from opposite-sign flanks could be mediated by neurones with receptive fields oriented and positioned so as to receive stimulation from both target and a flank.

Yet even if this modification were to produce good quantitative predictions, there are other arguments against the transducer model. Most damaging is the fact that the shape of the masking function depends upon the spatial frequency content of the mask (Foley, 1994). In order to explain this phenomenon, researchers have recently promoted models of contrast gain control (Wilson & Humanski, 1993; Foley, 1994; Teo & Heeger, 1994; Watson & Solomon, 1997b). It is conceivable that a contrast-gain-control model will provide a better account of flank-induced facilitation than the transducer model.

Zenger and Sagi (1996) have shown that an elaborated contrast-gain-control model provides a good fit to their flank-induced masking and facilitation results. Their model employs two successive filtering stages, separated by a nonlinearity. They claim, 'since first-stage (linear) filters are insensitive to masks of opposite phase...(our) results require a second processing stage to be incorporated into the model'. However, as we have shown here, facilitation from opposite-sign flanks can indeed be modelled with a single stage of filtering. It remains to be seen whether or not a single-stage contrast-gain-control model, such as those cited above, can account for the results of flank-induced masking and facilitation experiments.

Acknowledgements

References

Bowen, R. W., & Cotton, J. K. (1993). The dipper and bumper: pattern polarity effects in contrast discrimination. *Investigative Ophthalmology and Visual Science* (Suppl), *34*(4), 708.

Dresp, B. (1993). Bright lines and edges facilitate the detection of small line targets. *Spatial Vision*, *7*, 213–225.

Foley, J. M. (1994). Human luminance pattern mechanisms: masking experiments require a new model. *Journal of the Optical Society of America A*, *11*(6), 1710–1719.

Foley, J. M., & Boynton, G. M. (1993). Forward pattern masking and adaptation: effects of duration, interstimulus interval, contrast, and spatial and temporal frequency. *Vision Research*, *33*(7), 959–980.

Kapadia, M. K., Ito, M., Gilbert, C. D., & Westheimer, G. (1995). Improvement in visual sensitivity by changes in local context: parallel studies in human observers and in V1 of alert monkeys. *Neurone*, *15*, 843–856.

Legge, G. E., & Foley, J. M. (1980). Contrast masking in human vision. *Journal of the Optical Society of America*, *70*(12), 1458–1471.

Legge, G. E. (1981). A power law for contrast discrimination. *Vision Research*, *21*, 457–467.

Morgan, M. J., & Dresp, B. (1995). Contrast detection facilitation by spatially separated targets and inducers. *Vision Research*, *35*(8), 1019–1024.

Nachmias, J., & Sansbury, R. (1974). Grating contrast: discrimination may be better than detection. *Vision Research*, *14*, 1039–1042.

Polat, U., & Sagi, D. (1994). The architecture of perceptual spatial interactions. *Vision Research*, *34*(1), 73–78.

Polat, U., & Sagi, D. (1993). Lateral interactions between spatial channels: suppression and facilitation revealed by lateral masking experiments. *Vision Research*, *33*(7), 993–999.

Ross, J., & Speed, H. D. (1991). Contrast adaptation and contrast masking in human vision. *Proceedings of the Royal Society of London*, *246*, 61–69.

Solomon, J. A., & Watson, A. B. (1996). Cinematica: A system for calibrated, Macintosh-driven displays from within Mathematica, Behavior Res Methods. *Instruments and Computers*, *28*(4), 607–610.

Stromeyer, C. F. III, & Klein, S. (1974). Spatial frequency channels in human vision as asymmetric (edge) mechanisms. *Vision Research*, *14*, 1409–1420.

Teo, P. C., & Heeger, D. J. (1994). Perceptual image distortion. Paper presented at the SPIE Proceedings (pp. 127–141). Bellingham, WA: SPIE Press.

Watson, A. B., & Pelli, D. G. (1983). QUEST: a Bayesian adaptive psychometric method. *Perception and Psychophysics*, *33*(2), 113–120.

Watson, A. B., & Solomon, J. A. (1997a). Psychophysica: mathematica notebooks for psychophysical experiments. *Spatial Vision*, *10*, 447–466.

Watson, A. B., & Solomon, J. A. (1997b). Model of visual contrast gain control and pattern masking. *Journal of the Optical Society of America A*, *34*(9), 2379–2391.

Wilson, H. R., & Humanski, R. (1993). Spatial frequency adaptation and contrast gain control. *Vision Research*, *33*, 1133–1149.

Wilson, H. R., McFarlane, D. K., & Phillips, G. C. (1983). Spatial frequency tuning of orientation selective units estimated by oblique masking. *Vision Research*, *23*(9), 873–882.

Wolfram, S. (1996). *The mathematica book*, 3rd. Cambridge: Wolfram Media/Cambridge University Press.

Yang, J., & Makous, W. (1995). Modeling pedestal experiments with amplitude instead of contrast. *Vision Research*, *35*(14), 1979–1989.

Yu, C., & Levi, D. M. (1997). Spatial facilitation predicted with end-stopped spatial filters. *Vision Research*, *37*(22), 3117–3128.

Zenger, B., & Sagi, D. (1996). Isolating excitatory and inhibitory nonlinear spatial interactions involved in contrast detection. *Vision Research*, *36*(16), 2497–2514.